

Syracuse University

SURFACE

Physics

College of Arts and Sciences

2006

Hole Mobilities and the Physics of Amorphous Silicon Solar Cells

Eric A. Schiff
Syracuse University

Follow this and additional works at: <https://surface.syr.edu/phy>



Part of the [Physics Commons](#)

Recommended Citation

"Hole mobilities and the physics of amorphous silicon solar cells," E. A. Schiff, *J. Non-Cryst. Solids* 352, 1087-1092 (2006).

This Article is brought to you for free and open access by the College of Arts and Sciences at SURFACE. It has been accepted for inclusion in Physics by an authorized administrator of SURFACE. For more information, please contact surface@syr.edu.

Section 8. Electronic transport

Hole mobilities and the physics of amorphous silicon solar cells

E.A. Schiff *

Department of Physics, Syracuse University, Syracuse, NY 13244-1130, USA

Available online 13 March 2006

Abstract

The effects of low hole mobilities in the intrinsic layer of pin solar cells are illustrated using general computer modeling; in these models electron mobilities are assumed to be much larger than hole values. The models reveal that a low hole mobility can be the most important photocarrier transport parameter in determining the output power of the cell, and that the effects of recombination parameters are much weaker. Recent hole drift-mobility measurements in a-Si:H are compared. While hole drift mobilities in intrinsic a-Si:H are now up to tenfold larger than two decades ago, even with recent materials a-Si:H cells are low-mobility cells. Computer modeling of solar cells with parameters that are consistent with drift-mobility measurements give a good account for the published initial power output of cells from United Solar Ovonic Corp.; deep levels (dangling bonds) in the intrinsic layer were not included in this calculation. Light-soaking creates a sufficient density of dangling bonds to lower the power from cells below the mobility limit, but in contemporary a-Si:H solar cells degradation is not large. We discuss the speculation that light-soaking is ‘self-limiting’ in such cells.

© 2006 Elsevier B.V. All rights reserved.

PACS: 84.60.Jt; 72.20.Fr; 72.20.Jv; 71.23.Cq

Keywords: Silicon; Solar cells; Conductivity

1. Introduction

The device physics of pin solar cells involves – at a minimum – three different materials as well as the interfaces between them. Since the invention of hydrogenated amorphous silicon (a-Si:H) pin solar cells about thirty years ago, an enormous effort by scientists around the world has generated a correspondingly large number of papers detailing the optoelectronic properties of the materials. There have also been a number of pioneering efforts to integrate this information into models for the device physics of the cells [1–6]. The task of achieving useful insight when models have dozens of relevant parameters is daunting, and it is probably fair to say that there is no consensus understanding about how the cells work.

In this paper we first describe the *hole-mobility limit* of the efficiency for pin solar cells with absorber layers. Such a limit, which typically applies when hole drift-mobilities

are less than around $1 \text{ cm}^2/\text{Vs}$, is implicit in any of the device models for a-Si:H, but has been little explored since seminal work of Crandall [1]. The remarkable aspect of the hole-mobility limit is that it depends quite weakly upon processes that might seem more important, including photocarrier recombination and electron mobilities (which are assumed to be much larger than the hole mobilities).

For intrinsic a-Si:H, we summarize the many measurements of hole drift-mobilities; these mobilities are very low (typically less than $10^{-2} \text{ cm}^2/\text{Vs}$), although there have been promising reports of better mobilities. These mobility measurements are sufficient to establish a ‘hole mobility limit’ for single-junction cells with an a-Si:H intrinsic layer, and we show that a-Si:H nip solar cells prepared at United Solar Ovonic Corp. have achieved solar conversion efficiencies that are very close to the hole mobility limit. This achievement is a remarkable one. It implies that dangling bond densities have been kept low enough that they do not dominate the drift of holes, and that the n and p layers are good enough to act as nearly ideal electrodes to the cell.

* Tel.: +1 315 443 3901; fax: +1 315 443 9103.

E-mail address: [easchiff@syr.edu](mailto: easchiff@syr.edu)

These conclusions apply to the ‘as-deposited’ state of the cells. In use, a-Si:H based solar cells are light-soaked. Plausibly, the dangling bond density in the cells rises sufficiently to reduce the output power below the hole-mobility limit. The saturated degradation is about 30% for thick single-junction cells that lack optical enhancements such as back reflectors and texturing; the decline is less in optimized cells. The conclusion that the as-deposited cells are near their hole mobility limit then creates a puzzle, for it seems an unlikely coincidence that the light-soaking process should saturate just when cells show noticeable (30% or less) degradation. We therefore speculate that the light-soaking process is ‘self-limiting’ in the cells we have studied, and we discuss an obvious – but insufficient – mechanism for self-limitation in the concluding section.

2. Hole-mobility limit for pin solar cells

Perhaps the most elementary model for a pin solar cell assumes uniform photogeneration G in the intrinsic layer, and describes transport and recombination in this layer using only hole and electron mobilities μ_p and μ_n and an interband recombination coefficient b_R . For sufficiently low hole mobility $\mu_p \ll \mu_n$, and ideal n and p layers, this model yields a fairly simple approximation for the maximum power density from a thick cell [7]:

$$P = \left(\frac{2}{3}V_{OC}\right)^{3/2} \left(\mu_h \varepsilon (eG)^3\right)^{1/4}, \quad (1)$$

where the open-circuit voltage V_{OC} is given by

$$eV_{OC}^0 = E_G + k_B T \ln \left(\frac{G}{b_R N_C N_V} \right), \quad (2)$$

E_G is the bandgap of the material, N_C and N_V are the band-edge densities-of-states, e is the fundamental charge, k_B is Boltzmann’s constant, and T is the temperature (in Kelvin). ε is the permittivity of the absorber (SI units); we use the value $\varepsilon = 1.05 \times 10^{-10} \text{ C}^2/\text{N m}^2$ that is typical of a-Si:H.

The expression for V_{OC} is independent of the carrier mobilities. This aspect is important, and is fairly readily understood from the perspective that eV_{OC} reflects the splitting of the electron and hole quasi-Fermi levels E_{Fn} and E_{Fp} in the intrinsic layer [7]. By definition, $E_{Fp} = E_V - k_B T \ln(p/N_V)$; a similar relation holds for E_{Fn} . These expressions are not directly related to mobilities. The same perspective accounts for V_{OC} ’s logarithmic dependences upon b_R , N_C , and N_V .

The expression for the power density P depends directly only on the 1/4 power of the hole mobility μ_p and the 3/4 power of the generation rate G . It has a weak dependence upon recombination parameters through V_{OC} .

These analytical expressions are based on an approximate analysis that neglects the roles of diffusion. It is thus important to confirm them using a full numerical study of the same physical model. The black lines in Fig. 1 illustrate calculations of P done using the AMPS-1D computer code

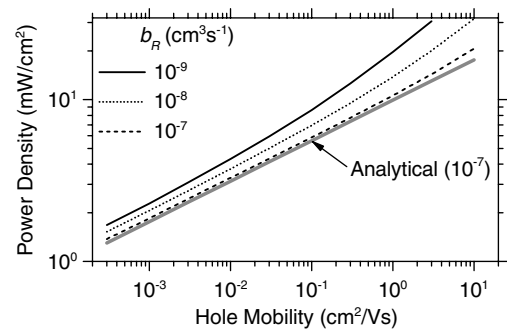


Fig. 1. Calculations of the power density from a thick pin solar cell as a function of the hole mobility for uniform photogeneration $3.3 \times 10^{20} \text{ cm}^3/\text{s}$. Numerical calculations for three values of the recombination coefficient b_R are shown as black lines; the gray line is from an analytical expression (Eq. (1)) using $b_R = 10^{-7} \text{ cm}^3/\text{s}$.

[4] for $G = 3.3 \times 10^{20} \text{ cm}^{-3}/\text{s}$, which was selected because it has the same magnitude that solar illumination makes in a-Si:H. Results are shown for three values of the interband recombination coefficient b_R [8]; the value appropriate for a-Si:H (see Section 4) is around $b_R = 10^{-9} \text{ cm}^3/\text{s}$. The gray line is the analytical approximation (Eq. (1)) for $b_R = 10^{-7} \text{ cm}^3/\text{s}$. Eq. (1) gives a good approximation to the full computer simulation over this range of hole mobilities. For larger values of μ_h , the power is larger than expected from Eq. (1); the increase reflects the increased importance of ambipolar diffusion, which was neglected in deriving Eq. (1).

Fig. 2 presents profiles of the ‘collection efficiency’ $1 - R/G$ (R is the recombination rate at a particular position x) and of the electric field as they were calculated for the maximum power point using the AMPS-1D code. The simulations were done for very thick absorber layers (30 μm); photocarrier collection is only significant in the p/i interface region that is illustrated. The profiles on the left-hand side are calculated for a low hole mobility $0.003 \text{ cm}^2/\text{Vs}$. These graphs illustrate that the electric field is confined to a fairly narrow region (width d_c) near the p/i interface. In addition, the photocarrier collection efficiency is only significant within this ‘collection width’, from which one draws the inference that the field-assisted drift of holes dominates the cell. This conclusion is consistent with the small magnitude of the ambipolar diffusion length $L_{\text{amb}} = \sqrt{2(k_B T/e)\mu_p \tau_R}$ for this mobility; for the present model $\tau_R = (Gb_R)^{-1/2}$. The two profiles on the right side of the figure illustrate the solutions for a much larger hole mobility $3 \text{ cm}^2/\text{Vs}$. For the smallest recombination coefficient $b_R = 10^{-9} \text{ cm}^3/\text{s}$, photocarrier collection is dominated by ambipolar diffusion. The low-mobility behavior is restored for $b_R = 10^{-7} \text{ cm}^3/\text{s}$, as can also be inferred from Fig. 1.

3. Hole drift-mobilities in a-Si:H

Fig. 3 shows the drift-mobility of holes near room-temperature for four a-Si:H samples. ECD94 is a plasma-

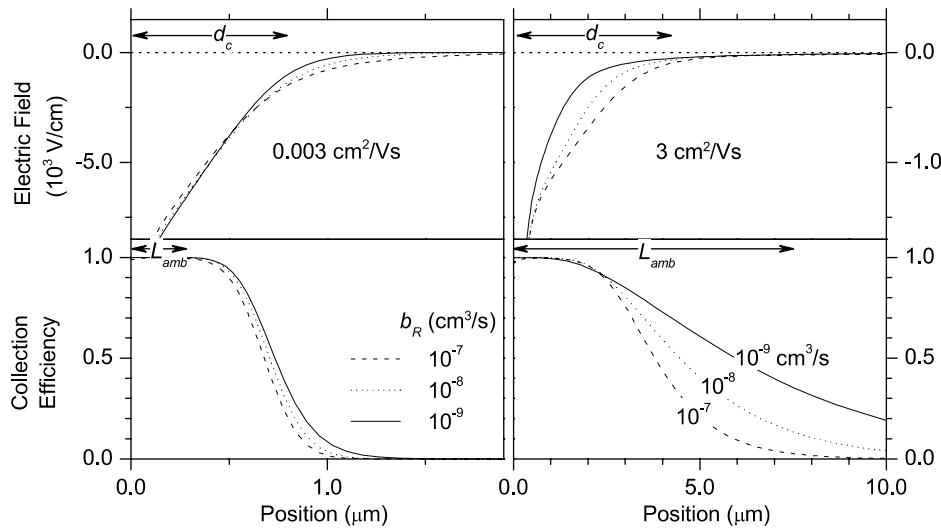


Fig. 2. Calculations of the profiles for the photocarrier collection efficiency $1 - R/G$ and the electric field at the maximum power point for a simple model of a pin solar cell; $G = 3.3 \times 10^{20} \text{ cm}^{-3}/\text{s}$. Graphs on the left side of the figure are calculated using a hole mobility of $0.003 \text{ cm}^2/\text{Vs}$; the three curves show these profiles for 3 values of the recombination coefficient b_R . Note that a factor 100 change in b_R has little effect on the profiles. The graphs also illustrate the field-assisted collection length d_c and the ambipolar diffusion length L_{amb} for $b_R = 10^{-9} \text{ cm}^3/\text{s}$; the small effects of b_R and the inequality $L_{amb} < d_c$ are important characteristics of the low-mobility limit. Graphs on the right side illustrate similar calculations for a cell with a higher hole mobility ($3 \text{ cm}^2/\text{Vs}$) for which the low-mobility characteristics are less evident.

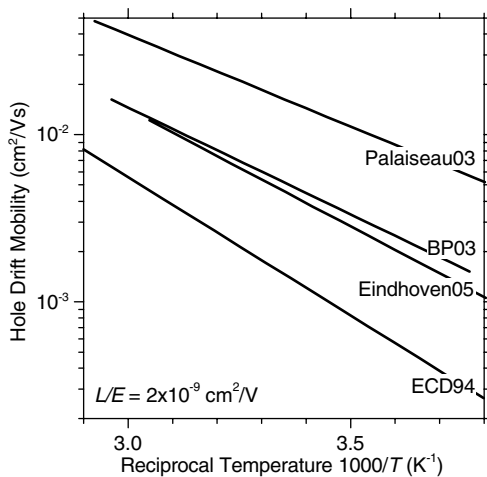


Fig. 3. Hole drift-mobility measurements as a function of temperature for five a-Si:H samples evaluated at a displacement-field ratio $L/E = 2 \times 10^{-9} \text{ cm}^2/\text{V}$. Definitions of the sample codes are given in the text.

deposited sample prepared around 1989; its hole drift-mobility is about the same as was reported for other samples prepared in the 1980's [9]. BP03 is a plasma-deposited material prepared fairly recently that used hydrogen-diluted silane as the source gas [10]. Eindhoven05 was prepared using the expanding thermal plasma method [11], and Palaiseau03 is a 'polymorphous' sample [12]. It seems apparent that hole drift-mobilities in a-Si:H have increased in the last decade. It is not clear at present how each of the changes in deposition procedures (hydrogen dilution, pressure, reactor design) has contributed to this improvement.

For solar cell applications, the most significant aspect of this graph is that the magnitudes of the drift-mobilities for

recent samples range from 6×10^{-3} to $2 \times 10^{-2} \text{ cm}^2/\text{Vs}$ at 300 K. Casual inspection of Fig. 1 indicates that the maximum power densities for cells with such mobilities are roughly the same as for a-Si:H single-junction solar cells; simplified cells that do not exploit 'optical engineering' (light-trapping and advanced back reflectors) typically have an initial power density of $7 \text{ mW}/\text{cm}^2$ under a solar simulator [13]. We show results from a more accurate model for a-Si:H in the next section.

We digress briefly to discuss the construction of Fig. 3. It is not common to present drift-mobilities for different materials and from different laboratories on a single graph. The reason for this is the 'dispersive' property of hole drift in a-Si:H and most other low-mobility semiconductors. Measurements of the photocarrier 'time-of-flight' t_T yield estimates of a drift-mobility through the expression:

$$\mu_d \equiv \frac{d^2}{2Vt_T}, \tag{3}$$

where d is the sample thickness and V is the bias voltage used in the measurement [14]. Experimentally, these drift-mobility estimates depend significantly upon the voltage that is applied; although rarely performed, the estimates also depend upon thickness. It is not obvious how to compare different materials except using the cumbersome approach of arranging for samples of identical thickness measured at some particular voltage.

This voltage-dependence of μ_d does not imply that photocarrier transport is nonlinear with electric field E . The displacement $x(t)$ of a sheet of carriers over a time interval t does (usually) depend linearly upon E . The voltage dependence is instead a consequence of 'dispersive transport' [15], which is evidenced in the power-law decays

of the photocurrent transients used to measure the transit times. It can be shown fairly generally that the drift-mobility μ_d depends only on the ‘displacement field ratio’ L/E [16]. Different materials can thus be compared – even in the presence of dispersive transport – at common values of L/E , and this was done to prepare Fig. 3 [17]. The lines shown in Fig. 3 are actually best-fits to the temperature-dependent hole drift-mobilities over the range of temperatures illustrated.

4. Amorphous silicon nip solar cells

In order to account for the strongly temperature-dependent and dispersive character of hole drift-mobilities in a-Si:H, a model incorporating an exponential valence bandtail has long been used [18]. The bandtail states act as traps for holes and as recombination centers; such bandtail states are provided for by the commonly used modeling codes including AMPS-1D [4] and ASA [19]. The simplest version of the valence bandtail model requires two additional parameters beyond those already introduced. These are the width of the bandtail ΔE_v , and the valence bandtail trapping coefficient b_{vp} that describes capture of mobile holes by these traps.

In Fig. 4 we present a numerical calculation (AMPS-1D code) of the dependence of the power density of a-Si:H solar cells upon the thickness of the intrinsic layer for solar illumination. The electronic parameters of the model are presented in Table 1; they have been published previously [20]. The hole transport parameters μ_p , ΔE_v , and b_{vp} are consistent with two samples in the middle of the range of Fig. 3. The bandtail recombination parameter $b_{vn} = 10^{-9} \text{ cm}^3/\text{s}$ has been taken from two independent high-intensity photoconductivity measurements [21,22]. The valence bandtail density at the bandedge $g_v^0 = 6 \times 10^{21} \text{ cm}^{-3}/\text{eV}$ is not an independent parameter in the pres-

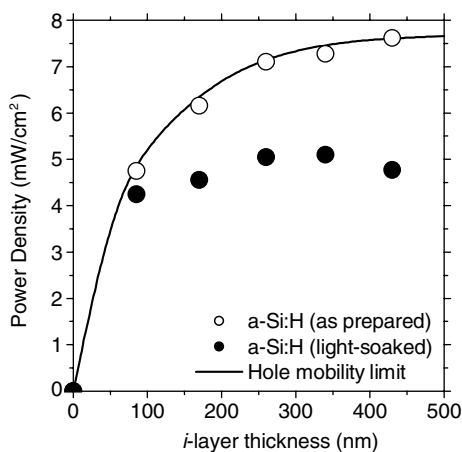


Fig. 4. Power output of a-Si:H nip solar cells for varying i -layer thicknesses (AM1.5 illumination). The symbols represent measurements on cells made at United Solar Ovonic Corp. [13]. The line is a computer calculation that illustrates the maximum power consistent with hole drift-mobility measurements (see text).

Table 1
a-Si:H solar cell modeling parameters [20]

μ_p	0.3 cm ² /Vs	Band-mobility of holes
ΔE_v	0.04 eV	Width of exponential valence bandtail
N_v	$4 \times 10^{20} \text{ cm}^{-3}$	Valence band effective density-of-states
b_{vp}	$1.3 \times 10^{-9} \text{ cm}^3/\text{s}$	Trapping coefficient $h^+ \rightarrow V^0$ (valence bandtail)
E_g	1.74 eV	Electrical bandgap
b_{vn}	$1.0 \times 10^{-9} \text{ cm}^3/\text{s}$	Trapping coefficient $e^- \rightarrow V^+$ (valence bandtail)
μ_n	2 cm ² /Vs	Band-mobility of electrons
ΔE_c	0.02 eV	Width of exponential conduction bandtail
N_c	$4 \times 10^{20} \text{ cm}^{-3}$	Conduction band effective density-of-states
b_{cn}	$1.3 \times 10^{-9} \text{ cm}^3/\text{s}$	Trapping coefficient $e^- \rightarrow C^0$ (conduction bandtail)

Solar cell performance is mainly sensitive to the boldfaced parameters.

ent model [7,20], but is needed for actual calculations. The bandedge parameters N_C and N_V were chosen to be consistent with measurements of the temperature-dependent open-circuit voltage measurements [20]. The bandgap E_G and the optical absorption spectra were consistent with direct optical measurements. Electron mobility and bandtail parameters are given for completeness, but the calculations are insensitive to the precise values shown.

For the present calculations, the apparent ‘hole mobility limit’ is the saturated value of the power found for very thick cells, which is about 7.6 mW/cm² for the present calculation. The value of the recombination parameter b_{vn} does have a slight effect on the calculation, as it did for the simpler model of Section 2. Decreasing b_{vn} by a factor 10 increases the saturated power by 6%. This percentage, calculated for white light illumination, is a bit misleading, since strongly absorbed green and blue photons are collected very readily. For red illumination, and more homogeneous absorption, reducing b_{vn} tenfold increases the power for thick cells by 13%. Increasing the hole band mobility μ_p tenfold increases the power for red illumination by 95%. These percentages are reasonably consistent with the results for the simpler model of Fig. 1, where one substitutes a typical hole drift-mobility of a-Si:H (around $10^{-2} \text{ cm}^2/\text{Vs}$ – see Fig. 3 at $T = 295 \text{ K}$) for the hole mobility parameter of the simpler model.

The experimental measurements of Fig. 4 are for a series of a-Si:H single-junction nip solar cells prepared at United Solar Ovonic Corp. [13]. The cells are deposited directly onto stainless steel substrates, which has a fairly low reflectivity. Production cells that are deposited onto textured, highly reflecting back contacts have larger power output. On the other hand, these simpler cells are fairly well suited to comparison with model calculations, and as can be seen in the figure, the ‘as-deposited’ cells agree reasonably well with the calculation. The light-soaked cells were exposed under open-circuit conditions for the unusually long time of 30 000 h, and of course have lower power output than the as-deposited cells.

The prediction of a saturated power for larger thicknesses may be surprising, since thickness series of a-Si:H based cells often show a peak power at some thickness followed by a decline. While this issue has not been defini-

tively studied, at least some of the ‘peaking’ is an optical effect due to use of a back reflector in optimized cells; modeling shows that cells with highly reflecting back contacts have a maximum in their power vs. thickness curve that is not seen with non-reflecting back contacts [23].

5. Discussion

The agreement between the measurements and calculations of Fig. 4 suggests that as-deposited a-Si:H single-junction solar cells from United Solar Ovonic Corp. have achieved their ‘hole mobility limit’. Cells at the hole-mobility limit must have defect densities that are low enough not to noticeably affect the power from the cells, and they must have p and n layers that are nearly ideal.

In of itself, Fig. 4 is not conclusive that the hole mobility limit has been reached for these cells. It is conceivable that the hole drift mobilities of these particular samples, which were not independently measured, were somewhat larger than expected from the parameters of Table 1, and that a density of dangling bonds present in the as-deposited sample then limits the saturated power.

We do believe that these samples from United Solar are near their hole-mobility limit. In recent work [24], we have measured the temperature-dependent properties of a thickness-series of similar single junction nip solar cells. Because the hole drift-mobility is strongly temperature dependent in a-Si:H (cf. Fig. 3), the temperature-dependent properties of the cells are a fairly definitive test for hole mobility limitation. One expects that the collection width should increase with temperature as the hole drift-mobility improves. We find satisfactory agreement between the temperature-dependent calculation and the measurements on as-deposited cells from 230 to 310 K. A noticeable discrepancy does set in for the higher temperatures, which we believe to be the onset of the effects of hole capture by dangling bonds (‘deep trapping’).

These conclusions concern the as-deposited state of a-Si:H, whereas it is the light-soaked state that is important in their usual application for solar power conversion. However, the conclusion that the as-deposited state is hole mobility limited creates an interesting perspective on light-soaking. As is evident in Fig. 4, the light-soaking effect in thick, single-junction cells saturates at about a 30% decline from the initial power. Dangling bond creation is the most plausible consequence of light-soaking, and it apparently continues until the density of dangling bonds is sufficient to modestly reduce the collection length of the cell (in the terminology of Fig. 2).

This coincidence is remarkable: saturation of the light-soaking effects in the cells we have studied seems to saturate just as the solar cells’ power begins to decline noticeably. A related observation is that open-circuit voltages V_{OC} in a-Si:H solar cells often change relatively little during light-soaking (0.05 V or less). We speculate that these coincidences are evidence for ‘self limitation’ of the light-soaking effect.

We have explored one obvious mechanism for such self-limitation. It is reasonable to assume that recombination of an electron with a hole trapped in the valence bandtail is the primary event underlying dangling bond creation. In a hole mobility limited cell, we expect this process to dominate the recombination traffic of an as-deposited cell. As the cell is light-soaked, the rate of creation will decline when recombination traffic ‘crosses over’ to a process involving holes trapped on dangling bonds. Our results, which are based on the ‘hydrogen collision’ model, indicate that the crossover effect provides a fairly good account for the kinetics of light-induced degradation in its initial stages, but they do not account for an ultimate saturation [25]. We are still seeking a more complete model.

Acknowledgments

The author thanks Howard Branz, Richard Crandall, Subhendu Guha, Jianjun Liang, Pauls Stradins, Baojie Yan, and Jeff Yang for many conversations and for the collaborations noted in the references. This research has been supported by the Thin Film Photovoltaic Partnership of the National Renewable Energy Laboratory.

References

- [1] R.S. Crandall, J. Appl. Phys. 55 (1984) 4418.
- [2] M. Hack, S. Guha, W. den Boer, Phys. Rev. B 33 (1986) 2512.
- [3] J.W. Park, R.J. Schwartz, J.L. Gray, G.B. Turner, in: Proc. of the 19th Photovoltaic Specialists Conference, IEEE, New York, 1988, p. 55.
- [4] H. Zhu, S.J. Fonash, in: R.E.I. Schropp et al. (Eds.) Amorphous and Microcrystalline Silicon Technology – 1998, Materials Research Society, Symp. Proc., vol. 507, Pittsburgh, 1998, p. 395.
- [5] R.E.I. Schropp, M. Zeman, Amorphous and Microcrystalline Silicon Solar Cells: Modeling Materials, and Device Technology, Kluwer, Boston, 1998.
- [6] U. Dutta, P. Chatterjee, J. Appl. Phys. 96 (2004) 2261.
- [7] E.A. Schiff, Solar Energy Mater. Solar Cells 78 (2003) 567.
- [8] Other parameters used in the calculations: $N_C = N_V = 5 \times 10^{20} \text{ cm}^{-3}$, $E_G = 1.8 \text{ eV}$, $\mu_n = 200 \text{ cm}^2/\text{Vs}$. See Ref. [7].
- [9] Q. Gu, Q. Wang, E.A. Schiff, Y.-M. Li, C.T. Malone, J. Appl. Phys. 76 (1994) 2310.
- [10] S. Dinca, G. Ganguly, Z. Lu, E.A. Schiff, V. Vlahos, C.R. Wronski, Q. Yuan, in: J.R. Abelson, G. Ganguly, H. Matsumura, J. Robertson, E.A. Schiff (Eds.), Amorphous and Nanocrystalline Silicon Based Films – 2003, Materials Research Society, Symp. Proc., vol. 762, Pittsburgh, 2003, p. 345.
- [11] M. Brinza, E.V. Emilianova, G.J. Adriaenssens, Phys. Rev. B 71 (2005) 115209.
- [12] M. Brinza, G.J. Adriaenssens, P. Roca i Cabarrocas, Thin Solid Films 427 (2003) 123.
- [13] S. Guha, in: R.A. Street (Ed.), Technology and Applications of Amorphous Silicon, Springer, Berlin, 1999, p. 252, The light-soaking measurements in Fig. 6.24 of this paper were done under open-circuit conditions (private communication with S. Guha).
- [14] For historical reasons dating to the earliest days of dispersive transport measurements, μ_d is often defined $\mu_d = d^2/V_T$ (i.e., without the factor of 2 of Eq. (3)). For consistency, in this paper we have recalculated published drift-mobilities that used this alternative definition.
- [15] H. Scher, M.F. Shlesinger, J.T. Bendler, Phys. Today 44 (1) (1991) 26.

- [16] Q. Wang, H. Antoniadis, E.A. Schiff, S. Guha, *Phys. Rev. B* 47 (1993) 9435.
- [17] For standard time-of-flight measurements, carriers have traversed half the sample's thickness at the transit-time, so $L = d/2$, and $L/E = d^2/2V$. Fig. 3 was prepared by estimating drift-mobilities at $L/E = 2 \times 10^{-9} \text{ cm}^2/\text{V}$ from the actual measurements of μ_d as a function of voltage.
- [18] T. Tiedje, in: J.D. Joannopoulos, G. Lucovsky (Eds.), *Hydrogenated Amorphous Silicon*, vol. 2, Springer, New York, 1984, p. 261.
- [19] M. Zeman, J.A. Willeman, L.L.A. Vosteen, G. Tao, W.J. Metselaar, *Solar Energy Mater. Solar Cells* 46 (1997) 81.
- [20] K. Zhu, J. Yang, W. Wang, E.A. Schiff, J. Liang, S. Guha, in: J.R. Abelson, G. Ganguly, H. Matsumura, J. Robertson, E.A. Schiff (Eds.), *Amorphous and Nanocrystalline Silicon Based Films – 2003*, Materials Research Society, Symp. Proc., vol. 762, Pittsburgh, 2003, p. 297.
- [21] G. Juska, J. Kocka, M. Viliunas, K. Arlauskas, J. Non-Cryst. Solids 164–166 (1993) 579.
- [22] P. Stradins, H. Fritzsche, P. Tzanetakis, N. Kopidakis, in: M. Hack et al. (Eds.), *Amorphous Silicon Technology – 1996*, Materials Research Society, Symp. Proc., vol. 420, Pittsburgh, 1996, p. 729.
- [23] X. Deng, E.A. Schiff, in: A. Luque, S. Hegedus (Eds.), *Handbook of Photovoltaic Science and Engineering*, John Wiley & Sons, Chichester, 2003, p. 505.
- [24] J. Liang, E.A. Schiff, S. Guha, B. Yan, J. Yang, *Appl. Phys. Lett.* 88 (2006) 063512.
- [25] J. Liang, E.A. Schiff, S. Guha, B. Yan, J. Yang, in: R.W. Collins, P.C. Taylor, M. Kondo, R. Carius, R. Biswas (Eds.), *Amorphous and Nanocrystalline Silicon Science and Technology – 2005*, Materials Research Society, Symp. Proc., vol. 862, Pittsburgh, 2005, p. A13.6.